Characterization of Reaction Intermediate Aggregates in Aniline Oxidative Polymerization at Low Proton Concentration

Zhongfen Ding,*,† Timothy Sanchez,‡ Andrea Labouriau,§ Srinivas Iyer,‡ Toti Larson,|| Robert Currier,⊥ Yusheng Zhao,# and Dali Yang*,§

Materials Physics and Applications Division, Bioscience Division, Materials Science and Technology Division, Earth and Environmental Science Division, Chemistry Division, and Los Alamos Neutron Scattering Center, Los Alamos National Laboratory, Los Alamos, New Mexico 87545

Received: March 23, 2010; Revised Manuscript Received: June 30, 2010

Aggregates of reaction intermediates form during the early stages of aniline oxidative polymerization whenever the initial mole ratio of proton concentration to aniline monomer concentration is low ($[H^+]_0/[An]_0 \leq 1.0$). Detailed characterization is carried out on those aggregates. The intermediate aggregates show a UV−Vis absorption peak at around 410 nm when dispersed in aqueous solution, whereas the peak is centered on 370 nm when dissolved in an organic solvent such as *N*-methylpyrrolidone. The electronic band gap decreases when the intermediates aggregate to form a solid, and thus, the absorption peak is red-shifted. Gel permeation chromatography (GPC) shows the aggregates contain a major low molecular weight peak with a long tail. The oligoanilines with low molecular weights consistently show a UV−Vis absorption peak at around 370 nm. Mass spectrometry confirms that the intermediate aggregates contain mainly a component with mass number 363 ($M + H^+$), likely a tetramer. UV−Vis, GPC, mass spectrometry, NMR, FTIR, and XRD characterization results are presented and chemical structures for the tetramer are proposed. The major components of the intermediate aggregates are likely highly symmetric phenazine- and dihydrophenazine-containing structures. These particular organic compounds have not been identified before as intermediates. The aggregation and precipitation of the tetramers apparently stabilizes these intermediates. The aggregates are highly crystalline, as evidenced by powder X-ray diffraction. A new reaction mechanism for the formation of these intermediates is proposed.

Introduction

Structured materials made from the conducting polymer polyaniline (PANI) have unique properties associated with their high surface area and ease of processing. The applications include antistatic and anticorrosion coatings,[1−3] sensors,[4,5] supercapacitors,[6,7] microelectronics,[8,9] batteries, and gas storage.[10,11] Thus, the link between synthesis conditions and PANI morphology has been investigated intensely in recent years. Factors known to affect PANI morphology include reaction temperature, aniline concentration, acid concentration, reactant ratios, mechanical disturbances, seeding strategy, and dopants.[12−15]

Aniline oxidative polymerization reaction can be carried out at different acid conditions, ranging from pH = 0 to pH = 11.[16,17] In recent years, it was discovered that aniline polymerization in aqueous solutions of a variety of weak acids or in water leads to PANI nanotube formation.[13,14,18,19] We recently showed that the initial proton-to-aniline mole ratio ($[H^+]_0/[An]_0$) affects PANI nanomorphologies and found that the formation of detectable intermediate aggregates is directly related to PANI nanotube formation,[20] consistent with the observations by others.[21] We found that the $[H^+]_0/[An]_0$ ratio is important in the polymerization kinetics due to aniline protonation (its conjugated acid has a pK_a of 4.87).[22] Whether the aniline monomer is fully protonated appears to determine the initial reaction pathway. Protonated aniline is slow to lose an electron to form a radical cation, whereas free aniline loses the electron easily.

When $[H^+]_0/[An]_0 > 1.0$, the intermediate aggregates were not detectable by UV−Vis, as was the case for the traditional PANI synthesis in strong acids.[23] When $[H^+]_0/[An]_0 \leq 1.0$, unprotonated aniline was oxidized quickly to form the intermediate aggregates that precipitated from the reaction suspension, thus slowing down further reaction.[20] These intermediate aggregates can form tetragonal rods when aggregating slowly or platelets when aggregation is fast.[20] By tuning the initial $[H^+]_0/[An]_0$ ratio, we slowed aggregation of the intermediates and demonstrated synthesis of nanotubes with rectangular cross sections.[24]

Aniline polymerization in pH-static conditions[25] differs from our reaction system in which pH naturally decreases as reaction proceeds. At the initial stage, the pH drops as aniline is oxidized in our system. When $[H^+]_0/[An]_0 < 1.0$, there is a very fast step during which intermediates form, followed by a decrease in the rate of intermediates formation. Under the pH-static condition, formation of the intermediates remains constant for a significant amount of time. Nevertheless, the pH condition for both the pH-static method and our simple synthesis system correlates well.[25] Specifically, $[H^+]_0/[An]_0 = 1.0$ corresponds to a point between pH = 2 and pH = 3 regarding the initial free aniline

* To whom correspondence should be addressed. (Z.D.) Address: MPA-11, MS D429, Los Alamos National Laboratory, Los Alamos, NM 87545. Fax: +1 505 665 4292. E-mail: zding@lanl.gov. (D.Y.) Address: MST-7, MS E549, Los Alamos National Laboratory, Los Alamos, NM 87545. Fax: +1 505 667 8109. E-mail: dyang@lanl.gov.

† Materials Physics and Applications Division.

‡ Bioscience Division.

§ Materials Science and Technology Division.

|| Earth and Environmental Science Division.

⊥ Chemistry Division.

Los Alamos Neutron Scattering Center.

10.1021/jp102623z
Published on Web 07/26/2010

SCHEME 1: The Chemical Structures of Some Organic Molecules Discussed in the Text

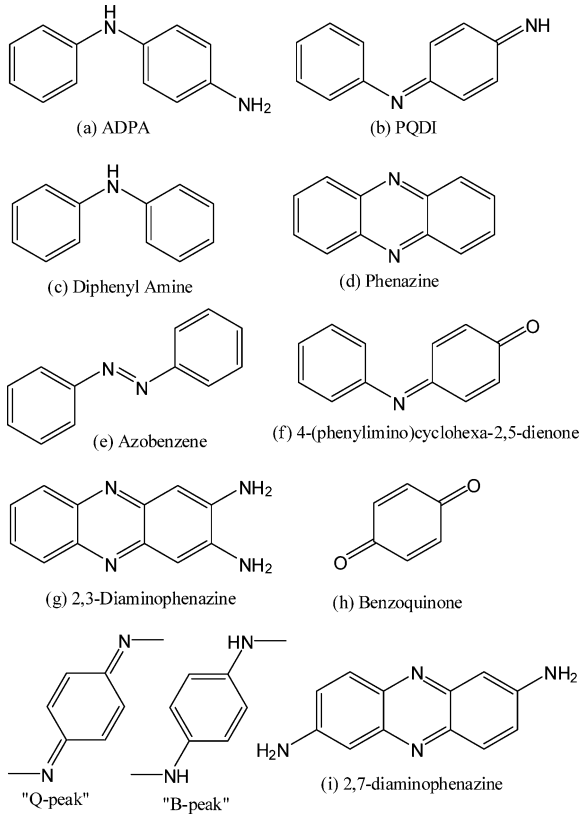

concentration; $[H^+]_0/[An]_0 < 1$ corresponds to the condition of pH = 4, 5, and 6; whereas $[H^+]_0/[An]_0 > 1$ corresponds to pH = 1.

The intermediate aggregates absorb at ~410 nm in situ.[20] This ~410 nm absorption peak is a single peak in the 300−1000 nm range, which is different from the broad band (~400−440 nm) observed together with the broad band at >600 nm for typical PANI emeraldine salt (ES) spectra.[26] This ~410 nm absorption was observed before and was considered to be *N*-phenylquinonediimine (PQDI, Scheme 1b).[17,27] This assignment was based on the results that PQDI can be synthesized by oxidizing aminodiphenylamine (ADPA, Scheme 1a) using freshly synthesized silver oxide,[28] and it has a UV−Vis absorption peak at ~428 nm.[29] We repeated the PQDI synthesis and characterized the ADPA and PQDI using both GC/MS and MALDI-TOF mass spectrometry as a reference. We found that the dimer ADPA (mass 184) was detectable by GC/MS, and both ADPA (mass $M^+ = 184$) and PQDI (mass $M + H^+ = 183$) were detectable by MALDI-TOF MS. However, in the intermediate aggregates from the aniline polymerization, no dimers were detected by either GC/MS or MALDI-TOF MS, which confirmed that the intermediate aggregates that absorbed at ~410 nm in aqueous reaction mixture were not likely to be PQDI (or ADPA).

The intermediate aggregates can be recovered by either centrifugation or filtration. We further found that the intermediate aggregates absorbed at ~370 nm when fully dissolved in an organic solvent, such as *N*-methylpyrrolidone (NMP), acetonitrile (ACN), or tetrahydrofuran (THF). Therefore, both the ~410 nm absorption in aqueous dispersion and the ~370 nm absorption in organic solvents are from the same intermediate aggregates. This finding is significant and may shed new light on previously reported results. For example, aniline polymerization products (dissolved in NMP) that absorb at ~370 nm have been synthesized and reported by different groups with quite different interpretation as to what the products are, ranging from linear tetramers,[30] to "azane" type structures,[31] to "*N*-phenyl phenazine and pseudomauveine" type structures,[14] and to macromolecules with "Michael-type addition on benzoquinone monoamine" structures.[32] Recently, Zujovic et al. isolated a reaction intermediate after 1 h into reaction, when the reaction suspension had a pH of 3.5. The intermediate was diluted and settled-out in water for 5 days. When dissolved in NMP, the intermediates also showed a UV−Vis absorption peak at 372 nm.[33] Alanine was added in the reaction, and as a result, the initial pH was close to neutral for their reaction. Many possible structures were eliminated, on the basis of ^{15}N NMR results, and an oxidized trimer structure ($C_{18}H_{13}N_3O$), with molecular weight of 287 was proposed.[33] Zujovic et al. expressed reservations on this proposed structure, noting the complexities in characterizing the various reaction products.[33]

Elucidating chemical structures of the intermediates is central to fully understanding aniline polymerization mechanisms. Due to multiple concurrent reactions, intermediate aggregates are expected to be a mixture of various species. However, the consistent UV−Vis absorption peak[20] suggests certain relatively stable chromophores exist in intermediate aggregates formed at the early stages of polymerization when the $[H^+]_0/[An]_0$ is less than 1.0. To probe these intermediates, their aggregates were separated after only 10 min of reaction (to avoid complexities associated with further reactions). Combined UV−Vis, GPC, GC/MS, ESI-MS, MALDI-TOF MS, NMR, FTIR, and XRD results for the intermediate aggregates are reported. The aggregates clearly consist of several major components although multiple other species (reaction products) are also present. Chemical structures of the major components of the intermediate aggregates and a formation mechanism are proposed on the basis of our analyses. The proposed tetramer structures are different from the related results in the literature.[14,30−33] The intermediate aggregates are quite stable as a solid phase and, thus, may be a significant part of many PANI products studied previously.[14,30−33] They may also be responsible for the specific properties of those PANI products, such as absorbing at ~370 nm when dissolved in NMP, specific FTIR peaks (~1414 cm^{-1}), or having crystalline X-ray diffraction peaks.[34] Structures for the major components of the intermediate aggregates are proposed without ruling out other possible structures (e.g., larger molecules, hydrolysis products, oxidized products etc) as the minor components.

Experimental Section

Reagents. Aniline (An), ammonium persulfate (APS) (ACS regent, 98+%), aminodiphenylamine (ADPA), HPLC grade *N*-methyl-2-pyrrolidone (NMP), and 60 Å silica gel for column chromatography were purchased from Sigma Aldrich. 1 N hydrochloric acid (HCl), ammonia, silicone gel flexible-backed thin layer chromatography (TLC) plates with fluorescent indicator, HPLC grade tetrahydrofuran (THF), methanol, acetonitrile, and cyclohexane were obtained from Fisher Scientific. Deionized (DI) water was used for all reactions and washing purposes. Aniline was vacuum-distilled prior to use.

Synthesis and Separation. Aniline polymerization at low $[H^+]_0/[An]_0$ (≤ 1.0) led to the formation of intermediate aggregates at the beginning of the reaction.[20] The goal of the synthesis was to control the concurrent reactions so that the intermediate aggregates formed while limiting subsequent reactions. The reaction intermediates were synthesized at three

different conditions: (a) $[H^+]_0/[An]_0 = 1$, specifically, 0.2 M aniline reacting with 0.05 M APS in 0.2 M HCl; (b) $[H^+]_0/[An]_0 = 0$, corresponding to 0.2 M aniline reacting with 0.05 M APS in DI water; (c) 0.2 M aniline reacting with 0.05 M APS in 0.1 M ammonia aqueous solution. After 10 min of reaction, 10 times by volume DI water was added into the reaction mixture to quench the reaction. Intermediate aggregates were then collected either through centrifugation or filtration. The intermediate aggregates were washed three times using DI water and vacuum-dried.

Instrumentation and Characterization. ***1. UV−Vis.*** A Cary 5000 spectrometer (Varian) was used for UV−Vis measurements. After washing, the intermediate aggregates were dispersed in DI water for UV−Vis measurements using DI water as the blank. The dehydrated aggregates were dissolved in various organic solvents for UV−Vis using the corresponding organic solvents as blanks. For the measurements in water/NMP mixtures, the corresponding solvent mixtures were used as blanks.

2. Gel Permeation Chromatography (GPC). The GPC consisted of an Alliance 2690 pump equipped with a Wyatt Rex differential refractive index detector and Waters 996 PDA detectors and two Polymer Laboratories PL Mixed B GPC columns. The temperature of the column was held at 60 °C. The injection volume was 100 μL, and the effluent flow rate was 1.0 mL/min. Molecular weights were estimated using retention times of polystyrene standards (Polymer Laboratories, Inc.) and Waters Corporation's Empower software. Washed and vacuum-dried samples were dissolved in NMP (with 0.01 M $LiBF_4$)[35] for GPC studies. The solution was filtered through a 0.45 μm Teflon filter prior to injection.

3. Gas Chromatography Mass Spectrometry (GC/MS). Analyses were performed using a Hewlett-Packard 6890 gas chromatograph (GC) interfaced with an Agilent 5975 inert source mass spectrometer detector (MS). The GC separation was performed on an Agilent J&W DB-WAXetr column (30 m × 0.32 mm, 0.50 μm film thickness) using high-purity helium as a carrier gas (average velocity, 49 cm/s; flow rate, 1.8 mL/min). The following GC temperature program was used: injector temperature, 250 °C; initial oven temperature, 100 °C; initial time, 5 min; temperature ramp, 10 °C/min up to 250 °C with a 40 min final holding time. The mass spectrometer ionization temperature was 250 °C, and the ionization energy was 40 eV. The column materials were observed to leach when NMP was used as solvent. Intermediate aggregates were thus dissolved in THF instead for the measurements. Aniline and ADPA were also dissolved in THF and measured by GC/MS as a reference and to set up the experimental conditions.

4. Electro Spray Ionization Mass Spectrometry (ESI-MS) and Matrix Assisted Desorption Laser Ionization Time-of-Flight Mass Spectrometry (MALDI-TOF MS). ESI-MS was performed on a Thermo LCQ-DECA. Samples were prepared in methanol/H_2O (1:1) and injected at a flow rate of 10 μL/min. The following conditions were used: capillary temp., 280 °C; spray voltage, 3 kV; sheath gas (N_2), 60 psi. MALDI-TOF MS was performed on a 4800 Plus MALDI-TOF TOF (Applied Biosystems, Framingham, MA) in positive ion, reflector mode. To avoid interference from matrix peaks, 1 μL of sample was directly spotted on 16 × 16 stainless steel sample plate, allowed to air-dry, and analyzed at varying laser intensities.

5. Liquid ^{1}H and ^{13}C Nuclear Magnetic Resonance (NMR). Experiments were performed at room temperature using a Bruker Avance NMR spectrometer operating at 300.13 MHz for ^{1}H and at 75.47 MHz for ^{13}C. Dimethylsulfoxide-d_6 (DMSO-d_6) was used as the NMR solvent and as an internal reference for the ^{1}H and ^{13}C chemical shifts.

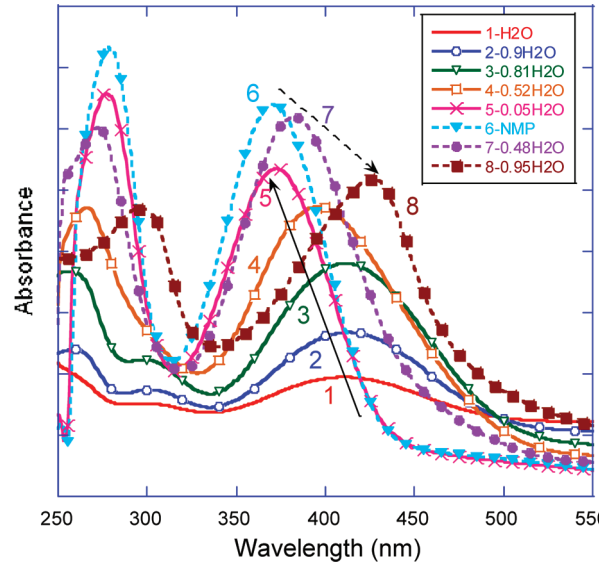

Figure 1. UV−Vis spectra of the intermediate aggregates dissolved in different H_2O/NMP mixtures. The solid lines start from a dispersion in water (line 1) with more and more NMP added into the dispersion (line 2 → 5). The dashed lines start from a solution in NMP (line 6) with more and more H_2O added in. The ratio are volumetric, for example, $0.9H_2O$ means 0.9/0.1 v/v of H_2O/NMP.

6. Fourier Transform Infrared (FTIR) spectroscopy. FTIR was directly measured on powder samples using a Thermo Nicolet FTIR instrument powered by OMNIC software.

7. X-ray Powder Diffraction (XRD). Data were obtained using a Siemens D5000 diffractometer. The diffractometer was equipped with a Huber Ge (220) cut curved crystal incident beam monochromator and operated at 50 kV accelerating voltage and 40 mA of beam current using Cu−Kα1 radiation.

8. Elemental Analysis. Elemental analysis was performed in Atlantic Microlab, Inc. (Norcross, GA). The H, C, N, and S measurements were accomplished by combustion analysis using automatic analyzers. Oxygen analysis was performed by pyrolysis. All analyses were percent by weight determinations.

Results and Discussion

1. UV−Vis Characterization. We recently reported that whenever the initial proton-to-aniline mole ratio is less than 1.0, the intermediate aggregates form at the early stage of aniline oxidative polymerization and have an absorption peak at ~410 nm.[20] Due to its poor solubility in water, the intermediate aggregates form a turbid dispersion in water that can easily be separated by centrifugation and filtration. On the other hand, the intermediates can completely dissolve in aprotic polar solvents (e.g., NMP, DMSO, THF, etc) and show an absorption peak at ~370 nm. We studied the UV−Vis absorption of the intermediate aggregates in solvents of different H_2O/NMP volumetric ratios and found that the absorption peak changes with solvent composition as shown in Figure 1. The solid curves were generated by adding increasing amounts of NMP to the aqueous dispersion. Since intermediate aggregates have poor solubility in water, the UV−Vis absorbance of the peak is low (line 1). The absorption peak does not change significantly when the water content is high (lines 1−3). As more NMP is added to the solution, more aggregates are dissolved, and finally, a transparent yellow-brownish solution is formed. The peak absorbance increases with increasing NMP concentration, and

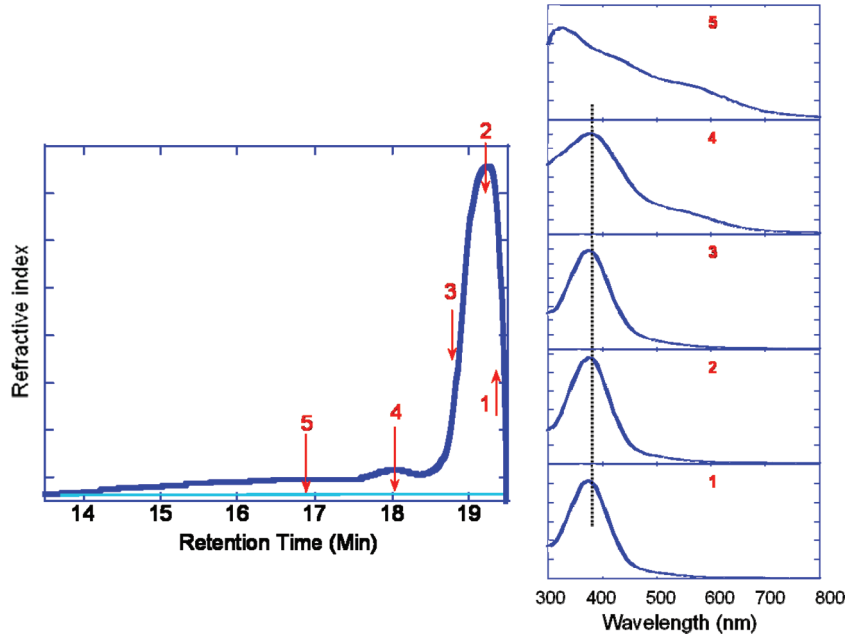

Figure 2. GPC result for the intermediate aggregates separated after 10 min of reaction. The major eluent is a small molecular peak (Mp ~ 320 using polystyrene standards). It has an absorption peak centered at ~370 nm. The eluent at position 4 (Mp ~ 1700) also has the 370 nm absorption peak, with the regular EB peaks emerging.

the peak blue-shifted to 370 nm (line 5). When we reversed this process, adding water to a concentrated NMP solution of the intermediate aggregates (dashed lines), the UV−Vis spectra showed that the peak red-shifted from 370 (line 6) to 420 nm (line 8).

These experiments suggest that the same intermediate aggregates absorb at ~370 nm in organic solvents but absorb at ~410 nm in aqueous dispersion. The 410 nm absorption peak was reported previously for aniline polymerization and was associated with aniline dimer PQDI.[16,27,29] Other research groups argue that the brown aniline polymerization product with UV−Vis absorption at around 420 nm is due primarily to the formation of branched structures.[36,37] Aniline polymerization products that dissolve in organic solvent and absorb at ~370 nm have also been reported with different assigned structures ranging from linear tetramer,[30] to azane type structure,[31] to macromolecules based on benzoquinoimine structure.[32] In Nalwa's study, the product absorbed at 370 nm in dimethyl formamide solution and absorbed at 430 nm when deposited on a glass slide.[30] The reaction was carried out in sulphanilic acid, a weak acid; thus, it is expected that a significant amount of the intermediate aggregates existed.[20]

Comparing the two cases when ~50 vol% of water is mixed with ~50 vol% of NMP, when the mixture starts from the water dispersion (line 4), it is not as well dissolved as when the mixture starts from the NMP solution (line 7). Since the measurement was carried out immediately after mixing, there may not have been enough time for the NMP molecules to break apart the aggregates in water to fully solvate them, thus making the peak slowly blue-shift on line 4. On the other hand, when the intermediates were first well dissolved in NMP, the absence of precipitation suggests that the intermediates have strong interactions with NMP solvent.

The intermediate aggregates formed at the three different acid conditions (as described in the synthesis part) have different morphologies, presumably due to different reaction kinetics.[20,24] Nevertheless, the intermediate aggregates show the same UV−Vis spectra whether dissolved in organic solvents such as NMP and THF or measured in situ in the reaction systems.

2. GPC Characterization. The typical molecular weight distribution for the intermediate aggregates is shown in Figure 2. The elution curve contains a low molecular weight peak (Mp ~320 relative to the polystyrene standard) with a long tail, which corresponds to the higher molecular weight components. All the UV−Vis spectra of the lower molecular weight components show the same UV−Vis absorption peaks centered at ~370 nm (curves 1−4) between 300 and 800 nm. For the higher molecular weight components, the UV−Vis spectra show a typical PANI EB spectrum with the absorption peaks centered at ~310 and ~630 nm. Although the molecular weight obtained from GPC is based on the polystyrene standards rather than an absolute number, the GPC results still provide insight into the molecular weight distribution. The intermediate aggregates mainly consist of small molecules, that is, oligoanilines. The long tail reflects the complications associated with multiple simultaneous reactions in the aniline polymerization process (including spontaneous reactions for further chain growth in NMP solution in air). This results in the presence of species with varying chain lengths.

All elution curves show a major low molecular weight peak at the same elution time with a long tail, although the tail part shows slight differences between samples synthesized at the three different acid conditions. The GPC results suggest a major component (~70 wt %) with a low molecular weight. This component has a UV−Vis absorption at ~370 nm. In addition, the oligoanilines possibly contain the same stable functional group (chromophore) that absorbs at ~370 nm even when the molecular weights are slightly higher (<1700 nominally from GPC). When the oligoanilines increase in chain length, a broad absorption at >600 nm appears due to the formation of longer conjugated structures.

3. Mass Spectrometry Characterization. The intermediate aggregates are a mixture of components because there are multiple concurrent reactions occurring. For such a mixture, elemental analysis is not a definitive method to determine composition. The measurements typically result in an average of all components in the mixture. Thus, we employed a mass spectrometry technique to probe the major components.

3.1. GC/MS Characterization. GC/MS conditions were optimized for the separation and detection of aniline and ADPA reference solutions. Aniline had a retention time of 15.211 min and preserved a primary molecular ion with a mass-to-charge ratio (*m*/*z*) value of 93 (M^+). In addition to aniline, a small peak was observed at a retention time of 15.784 min, the mass spectra of which matched that of the THF stabilizer, butylated hydroxyltoluene (BHT). For the ADPA in THF solution, ADPA eluted at a retention time of 43.799 min and preserved a primary molecular ion with a *m*/*z* value of 184 (M^+). BHT was also observed in this sample with a retention time of 15.784 min. In addition to BHT and the primary ADPA peaks, several small peaks that are impurities were observed including an eluent with a retention time of 20.068 min and a *m*/*z* value of 169 (M^+), which was identified as diphenylamine (Scheme 1c) and another eluent with a retention time of 42.204 min, with preserved molecular fragments with *m*/*z* values of 210, 195, 184, and 167, matching diaminophenazine molecules (Scheme 1g or i).

GC/MS with similar experimental conditions has been used to detect other related small molecules, such as benzoquinone (Scheme 1h), azobenzene (Scheme 1e), and substituted azobenzene etc.[38] Similar methods were used to conduct GC/MS analysis of our intermediate aggregates in THF solution. The eluent peaks appeared at identical times for the three different intermediate aggregates formed at (1) low acid, (2) aqueous (no acid), and (3) ammonia reaction conditions, which suggest that these intermediate aggregates appear to have similar chemical structures, compositions, and properties. There were a total of 15 eluent peaks from the intermediate aggregates solutions. The eluent with a retention time of 15.784 min matches BHT. Interestingly, the other eluents with different retention times have similar mass fragments, with each fragment having different abundances. For example, the eluent at 10.388 min consisted primarily of fragments with the *m*/*z* values of 355 and 267, whereas the eluent at 12.027 min was dominated by fragments with *m*/*z* values of 341 and 429, and the eluent at 12.948 min was dominated by fragments with *m*/*z* values of 281, 327, and 147. The major masses in all of these eluents included 73, 147, 221, 281, 327, 341, 355, and 429. The reason for formation of these fragments is most probably due to the cross-linking of the oligoanilines. It is well documented that the quinoneimine groups are highly reactive. The imine nitrogen cross-links with benzene ring to form a networked structure containing mainly tertiary amines at 140 °C in a diluted EB solution in NMP.[39] Although the cross-linking during the analysis prohibited the usage of the GC/MS characterization to study the main component of the intermediate aggregates, the GC/MS analysis ruled out some related small molecules as major components, such as benzoquinone, azobenzene, ADPA, phenazine (Scheme 1d), and *N*-phenyliminocyclohexa-2,5-dienone (Scheme 1 f). These molecules should have easily been detected if they were present.

3.2. ESI-MS and MALDI-TOF Characterization. Unlike the GC/MS, both ESI-MS and MALDI-TOF MS use soft ionization techniques at low temperature and, thus, can prohibit the reactions between the intermediate molecules. Figure 3 shows the ESI-MS spectra of the intermediate aggregates dissolved in 1:1 methanol/H_2O solvent. The major component of the intermediate aggregates had a *m*/*z* value of 363. There were also minor peaks with the *m*/*z* values such as 273, 289, 335, 379, 454, and 470. These minor components may be due to mass fragmentations or other species formed by further reaction of the intermediates. It is worth noting that the intermediate aggregates did not completely dissolve in 1:1 methanol/H_2O solvent, and thus, longer oligoanilines might not have dissolved. However, our primary interest is the major component corresponding to the low molecular weight GPC peak.

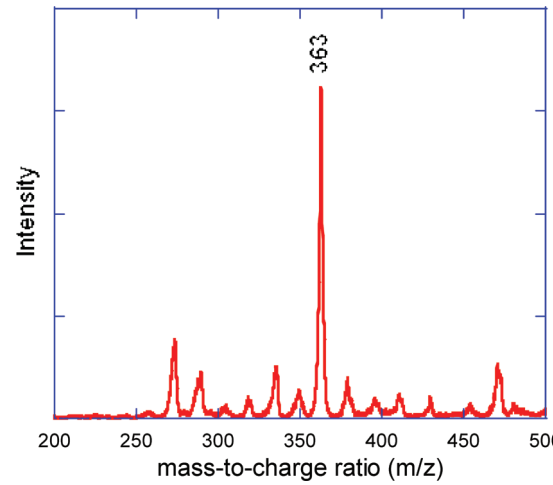

Figure 3. ESI-MS results for the intermediate aggregates dissolved in MeOH/H_2O (1:1). The major component has a mass number of 363, corresponding to a tetramer. There are minor impurities in the intermediate aggregates.

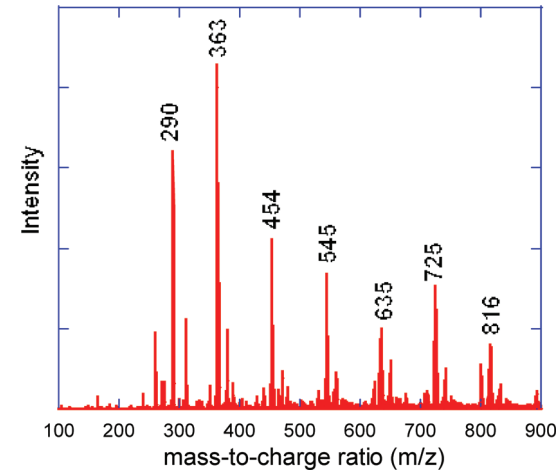

Figure 4. MALDI-TOF results for the intermediate aggregates that dissolved in THF. No matrix is added for the measurement to eliminate interference peaks. The major peak is also at mass number 363.

The MALDI-TOF MS measurements were performed without matrix to eliminate the interferences from common matrix molecules. The resolved MALDI-TOF MS spectrum appears to be more complicated than that of ESI-MS, as shown in Figure 4. Multiple peaks were detected with high mass resolution. Consistent with ESI-MS, the major peak also had the *m*/*z* value of 363, although other peaks with the *m*/*z* values of 290, 454, 545, 635, 725, and 816 were observed with significant intensity, as well. Control experiments showed that the MALDI-TOF results using freshly prepared solution were quite different from that obtained using a sample aged 1 day. The aged sample had many more peaks without a predominant peak. We suspect that cross-linking or chain growth when the intermediate aggregates were dissolved and then dried up led to the increase in the number of peaks and higher molecular weight components.

On the basis of the mass spectrometry and GPC results, we propose that the major components in the intermediate aggregates (>70 wt % from GPC results) are tetramers with a molecular weight of ~363. However, the intermediate aggregates also appear to contain multiple oligoanilines with

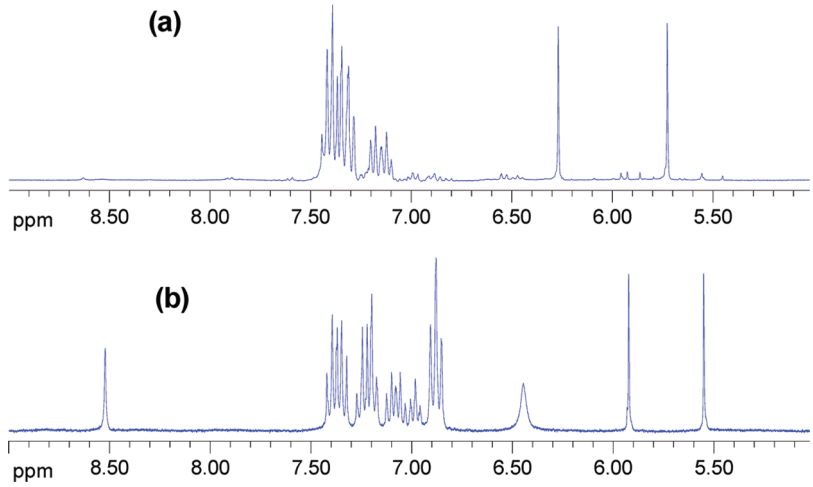

Figure 5. ^{1}H NMR spectra of (a) the intermediate aggregates and (b) a separated minor component.

different chain lengths. Dimers were not detected in the intermediate aggregates, suggesting that PQDI or two-ring molecules are not major components in the intermediate aggregates.

4. Liquid ^{1}H NMR and ^{13}C NMR Characterization. ^{1}H NMR spectra of the aggregates in DMSO-d_6 solution are shown in Figure 5a. The major peaks of the intermediate aggregates have chemical shifts at 7.4−7.3 (10H), 7.25−7.1 (4H), 6.27 (1H), and 5.72 ppm (1H). The ^{1}H signals with chemical shifts at 7.0−7.5 ppm (14H) are associated with protons directly bonded to aromatic rings. Since the observed chemical shifts are all <7.5 ppm, each aromatic ring may be directly bonded to amines. The sharp peaks at 6.27 and 5.72 ppm are characteristic of the intermediate aggregates. These sharp singlets appear to be a pair with a 1:1 ratio. A similar set of ^{1}H NMR peaks between 5.5 and 6.5 ppm was reported independently by Venancio et al. and assigned to substituted quinoneimine units.[31] Kriz and co-workers deduced that these were not N−H protons and also assigned these peaks to similar substructure "oxygen-containing substituted quinoneimine structure".[40] On the other hand, Cotarelo et al. assigned similar peaks (5.16 and 5.57 ppm singlets) to amine protons in their study of 2-ADPA polymerization.[41] It is not certain that these peaks can be readily assigned to N−H. The primary amine groups (−NH_2) easily form hydrogen bonding and, thus, usually have broad peaks. The secondary amine groups (−NH−), when connected to two aromatic rings, usually have a high chemical shift (>8 ppm). It is not clear that the two peaks observed in this work at 6.27 and 5.72 ppm can unambiguously be assigned to substituted quinoneimine units or to branched structures.

A series of organic molecules that contain quite similar structures have characteristic ^{1}H chemical shifts at 5.5−6.5 ppm. For instance, the C−H protons in diaryldihydrophenazines have chemical shifts at 5.8−6.3 ppm for the C−H protons next to the C−N on dihydrophenazine rings.[42] C−H groups in Mauveine dyes have chemical shifts of 5.9−6.3 ppm at similar positions, even though the detailed structure is considered to be *N*-phenylphenazinium-based.[43−45] The ^{1}H NMR study of safranine derivatives also shows that the neighboring amino groups and the *N*-phenyl substitution on the phenazinium ring lead to the C−H proton in between to resonate at 5.5−6.0 ppm.[46] N-Substitution appears to be critical for the C−H adjacent to the N−C to have a chemical shift reduced by ∼0.6−0.7 units.[46] Combining the mass spectroscopic results, we propose that these

SCHEME 2: Characteristic ^{1}H and ^{13}C [in brackets] NMR Data for the Tetramers[a]

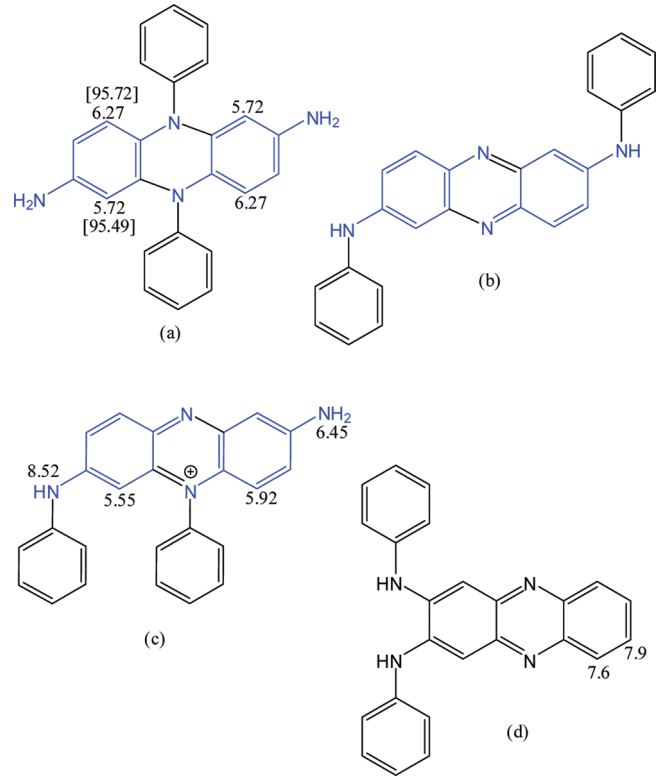

[a] The C−H protons not labeled have chemical shifts at ∼7.0−7.5 ppm.

two singlet peaks at 6.27 and 5.72 ppm belong to the tetramer, 5,10-diphenyl-5,10-dihydrophenazine structure, as shown in Scheme 2a.

The ^{13}C NMR (Figure 6) spectra are surprisingly clean, considering that the aggregates are a mixture of different components with the major component having a molecular weight of 363 (possibly a tetramer with 24 carbon atoms). The simplicity of the carbon lines suggests that the major components (tetramers) have symmetric structures. The ^{13}C lines at 95.49 and 95.72 ppm correspond to carbons connecting to the protons with chemical shifts of 5.72 and 6.27 ppm, respectively. The ^{13}C peaks at 120−130 ppm correspond to the C atoms in aromatic benzene rings that connected to other C atoms. The peaks around 140 ppm likely correspond to the C atoms on

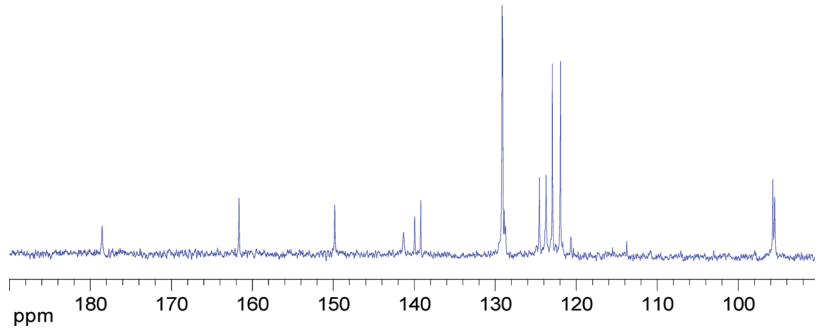

Figure 6. ^{13}C NMR for the intermediate aggregates.

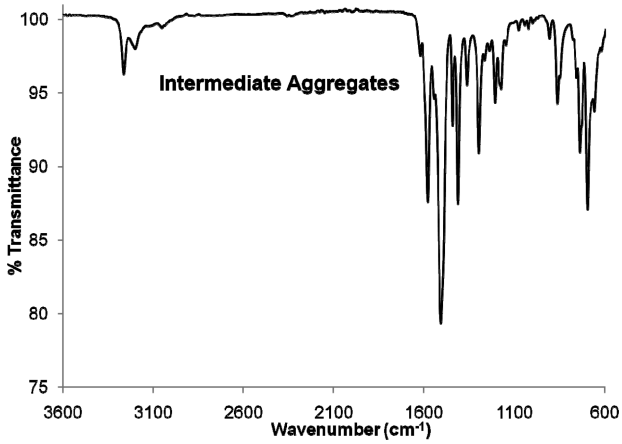

Figure 7. FTIR results of the powder of intermediate aggregates measured directly.

phenazine or hydrophenazine structures directly connected to N atoms. The peak at 150 ppm suggests carbon on a benzene ring directly connected to a nitrogen atom. The two peaks with very high chemical shifts may correspond to carbon atoms connected to the phenazinium N because the positively charged N atoms can attract electron clouds similar to what is seen with oxygen atom. However, these lines may be due to some larger oligomers with protonated quinoneimine structures.

5. FTIR Characterization. The FTIR spectra are shown in Figure 7. The plot includes the peaks typically seen in PANI EB structure:[47] (1) the 1582 cm^{-1} peak corresponding to the quinoid imine structure, (2) the 1502 cm^{-1} peak corresponding to the benzenoid amine structure, (3) the 1297 cm^{-1} peak due to C−N−C stretch vibration, and (4) the 1175 cm^{-1} for benzene C−H bending vibration. These peaks are similar to those found in the conventionally synthesized PANI EB (synthesized in strong acid),[47] which have much broader peaks at the similar wavenumbers. In addition, there are peaks at 1444 and 1413 cm^{-1}. The 1444 cm^{-1} is likely due to aromatic C−N vibration, and the 1413 cm^{-1} is possibly due to totally symmetric ring stretch of phenazine structure.[47] The relatively small 1363 cm^{-1} peak is likely due to a −C═N−C stretch vibration, and the 1208 cm^{-1} can be associated with aromatic C−H bending vibration. The peak at 862 cm^{-1} is due to a 1,2,4-substituted benzene ring, and 737 and 696 cm^{-1} are due to monosubstituted benzene structure. The peaks at 3264 and 3196 cm^{-1} are due to N−H asymmetric and symmetric stretching vibrations. All the FTIR peaks are accountable from the structures in Scheme 2.

On the basis of the presented UV−Vis, GPC, MS, NMR, and FTIR characterizations of the intermediate aggregates, we point out that the proposed structures in the literature conflict with one or more of our characterization results. For example, the phenyl capped linear tetramers have UV−Vis absorption peaks at ∼300 and ∼600 nm,[48−51] which are different from the ∼370 nm UV−Vis absorption consistently observed for the intermediate aggregates. In addition, linear tetramers have a ^1H NMR chemical shift at 7−8 ppm for both benzoid and quinoid groups and have secondary amine (−*N*−H) protons at ∼8.3 ppm and primary amine ($-NH_2$) protons at ∼5.5 ppm,[15,51] which are also different from our NMR data. Therefore, we do not presently believe that the tetramers have linear structures, as suggested by Nalwa's study.[30] For the azane type structures, as proposed by Venancio and co-workers,[31] and for the Michael type addition products based on benzoquinone monoamine as proposed by Surwade and co-workers,[32] there should obviously be strong FTIR absorption peak for the carbonyl group at 1650−1800 cm^{-1}. However, no absorption peak was observed at the 1650−1800 cm^{-1} region in the FTIR spectra of the intermediate aggregates. In addition, the ^{13}C NMR is far too simple for the polymer or macromolecular structures as proposed in these articles because those structures should have several dozens of ^{13}C lines. The wide variety of structures that often contain "*N*-phenyl phenazine and pseudomauveine" subunits as proposed by Stejskal and co-workers[14] are the closest to the structures that we present here. However, all the pseudomauveine, or phenasafranin, or *N*-phenyl phenazine are well-known purple dyes, which have UV−Vis absorption at 520−540 nm[43−45,52] but not at ∼370 nm, as we have observed in the UV−Vis characterization of the intermediate aggregates in organic solutions.

We suggest that the proposed tetramers have two main structures, as shown in Scheme 2a and b. Phenazine has a UV−Vis absorption at 368 nm.[53,54] The 2,7-diaminophenazine also has absorption at 370 nm.[55] In addition, when phenazine is mixed with dihydrophenazine, phenazhydrins form, which absorb similarly to phenazine.[56] This electronic absorption is due to $\pi \rightarrow \pi^*$ transitions. Substitution to the benzene rings on the phenazine structure does not strongly affect the absorption.[54] However, substitution on the N atoms forming the phenazinium structure leads to characteristic absorption at 500−540 nm, as for the mauveine type dyes.[44,54] The structures a and b thus match the UV−Vis results and can also account for the consistent ∼370 nm peak. These two structures are both symmetric, and as a result, the characteristic totally symmetric phenazine ring stretching vibration peak (1413 cm^{-1}) measured by FTIR is quite strong. All the FTIR peaks and major NMR peaks can also be accounted for in these structures. On the basis of the ^1H NMR peak integration, the ratio of structures a to b in the intermediate aggregates is approximately ∼1:1. The compound diphenyldiaminophenazine (b) has 16 C−H protons with a chemical shift of 7−7.5 ppm, whereas the compound diphenyldiaminodihydrophenazine (a) has 12 C−H protons with a chemical shift of 7−7.5 ppm, 2 C−H protons of 5.72 ppm, and 2 C−H protons of 6.27 ppm. A 1:1 ratio of the two

compounds matches the integrated results of 14H/1H/1H of the main peaks in ^{1}H NMR, as shown in Figure 5a. Zujovic and co-workers found that the intermediates should have only one type of imine nitrogen, on the basis of their ^{15}N NMR study, which is consistent with our proposed structures (b).[33]

In addition to these two major compounds, we propose two minor components shown as Scheme 2c and d. These two structures contribute to the small peaks detected in ^{1}H NMR (Figure 5a).

Chemical reaction mechanisms consistent with the observations were formulated. Scheme 3 shows several options for aniline polymerization and intermediate formation at low proton concentrations. The chemical reasoning behind these proposed mechanisms is as follows: Due to low proton concentration, free aniline molecules are quite easily oxidized into dimers in the oxidized PQDI form. Therefore, an appreciable amount of PQDI accumulates in the reaction system. Since the PQDI is quite reactive with APS as oxidant, the accumulation promotes rapid cross-linking to form tetramers. Whether a tetramer is in either the oxidized or reduced form depends on the stability of the tetramers. We suggest that there are at least three plausible cross-linking routes for forming tetramer structures: namely, a, b, and c, as shown in Scheme 3. In addition to the PQDI cross-linking, the PQDI can certainly react with free aniline molecules to form yet another tetramer structure (d). However, structure d was found to exist only in small amounts, according to the NMR analysis. Specifically, there were only minor components in ^{1}H NMR spectra corresponding to the C−H chemical shifts at ∼7.6 and ∼7.9 ppm as assigned in Scheme 2d. Additional work will be required to determine more precisely which mechanisms are dominant.

The tetramer molecules have strong $\pi-\pi$ interactions with poor solubility in water and, thus, form aggregates rapidly. The aggregation causes phase separation. The aggregates are relatively stable in aqueous solution or in anhydrate form. However, the aggregates are highly reactive when they dissolve in organic solvents. The presence of oxygen will promote oxidation and further reaction of the oligoanilines to form larger molecules, as well.

The complete separation of the intermediate contents proves to be very difficult due to the reactivity as observed during mass spectrometry measurements. TLC was tried for the separation, and different components were seen to be separated by forming separated lines. Yet, each line was not pure and showed higher molecular weight components with the *m*/*z* values of 545, 725 etc., indicating that further chemical reaction had been concurrent during the separation process. Silica gel column was also used for separating the intermediate aggregates for multiple times. Different components could be separated, but the complication of further reaction remained during the separation process or other handling processes (e.g., solvent evaporation, deposition). Therefore, the separated components always contained higher molecular weight peaks. Correspondingly, the ^{13}C NMR results show many more lines for the separated components than for the original intermediate aggregates collected from the aqueous reaction mixture. It was found that the oligoanilines were easily oxidized or react with each other when well-dissolved in organic solvents.

One component was separated and purified (after multiple runs of column chromatography) which appeared to be pure by MALDI-TOF measurement. The ^{1}H NMR for this component is shown as Figure 5b. Interestingly, the NMR data matches the set of small peaks when compared to Figure 5a. The ^{1}H NMR suggests that the structure of this component is as shown in Scheme 2c. The fact that structure c forms only in a small amount may be due to the bulky benzene rings repelling each other at this position (Scheme 3c) and, thus, inhibiting cross-linking reactions. Clearly, to obtain pure intermediate aggregates, extreme care is needed. An improved separation technique (e.g., handling the separation under inert atmosphere) is definitely needed.

SCHEME 3: Formation Mechanism of the Intermediate Aggregates at Low Initial Proton Concentrations ($[H^+]_0/[An]_0 \leq 1.0$)

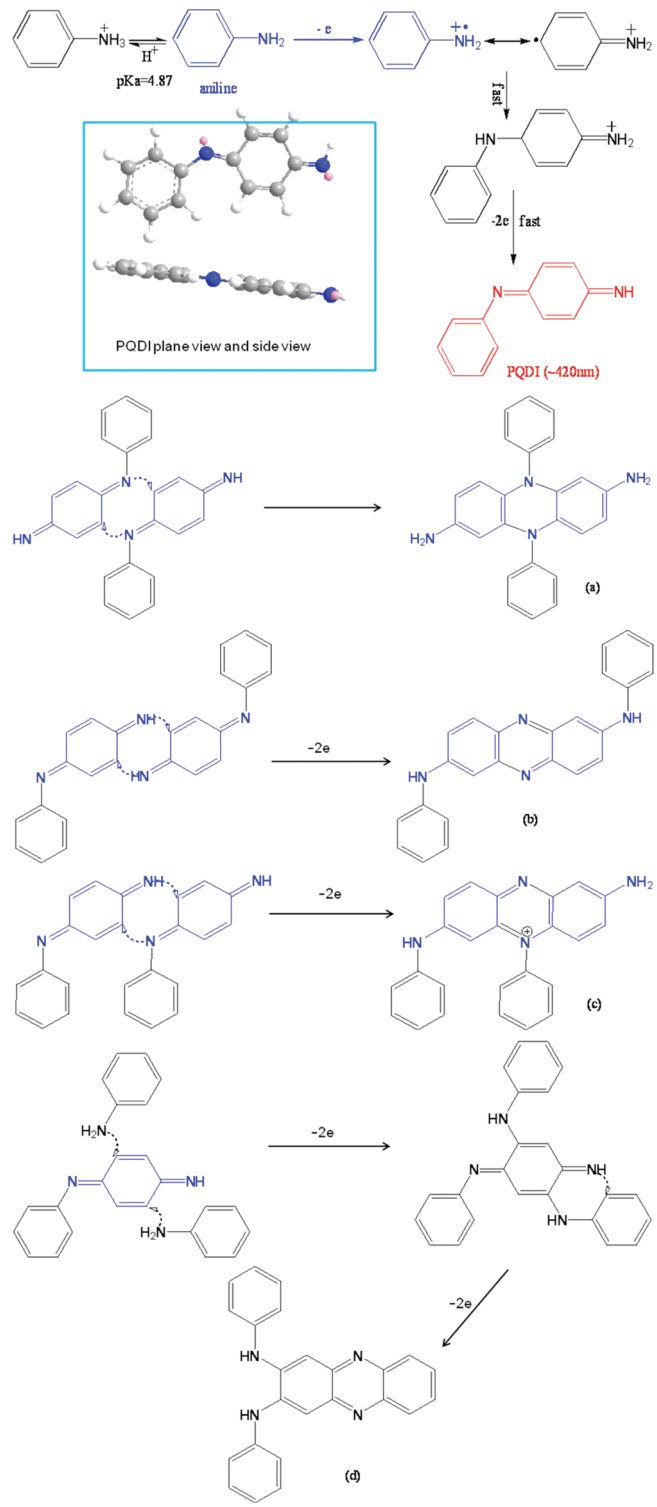

6. XRD Characterization. The powder XRD pattern of the intermediate aggregates powder is shown in Figure 8. The

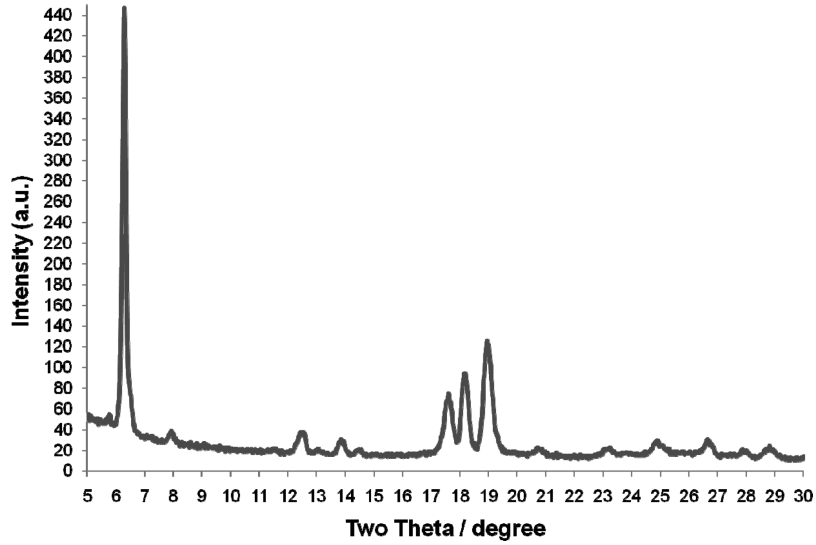

Figure 8. Powder X-ray diffraction patterns of the intermediate aggregates.

aggregates formed highly crystalline structures. The XRD pattern shows a major peak with a 2θ value of 6.28°, corresponding to a d value of 14.07 Å. This indicates a preferred orientation, possibly a one-dimensional preference due to strong $\pi-\pi$ interaction of the chromophore functional group. XRD peaks at 6.28° have been observed before in PANI products.[34] The intermediates should be the origin of the detected crystallinity in PANI products.

7. Elemental Analysis. The samples were filtered, washed, and dried under ambient conditions after isolation. A full elemental analysis of H, C, N, O, and S indicated that the formula for the intermediates mixture should be $C_{6.18}H_{5.09}N_1O_{0.30}$, with S at 0.02 at. %. The S is most likely from SO_4^{2-} ion adsorption. Thus, we propose the intermediate tetramers have the atomic ratios (formulas) C_6H_6N ($C_{24}H_{20}N_4$) or $C_6H_{4.5}N$ ($C_{24}H_{18}N_4$), which corroborates our comprehensive study results. The small amount of oxygen detected in the mixture could well be due to hydrolysis of quinoid

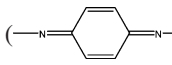

structures into benzoquinone imine

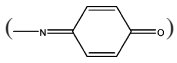

structures.

Conclusion

The intermediate aggregates formed at the early stage of aniline chemical oxidative polymerization at low initial proton concentrations were characterized using UV−Vis, GPC, ESI-MS, MALDI-TOF, ^{1}H and ^{13}C NMR, FTIR, and XRD. It appears that the intermediate aggregates contain tetramers as major components. The tetramers consist of mainly symmetric diphenyldiaminophenazine and diphenyldiaminodihydrophenazine structures with a ratio of ~1:1. These chromophores led to a consistent UV−Vis absorption at ~370 nm when dissolved in organic solvents. The symmetric planar structures of these molecules also led to strong $\pi-\pi$ interactions, accounting for their poor solubility in water, phase segregation, and packing into a solid crystalline structure.

The aggregates are relatively stable in aqueous dispersion or after drying. However, the aggregates are highly reactive when well dissolved in organic solvents. Oxygen in air promotes further oxidation of the oligoanilines to form larger molecules. Therefore, separation and purification of each component remains a challenge using traditional TLC and column chromatography because the separated components appear to have a wider range of distinct species (reaction products) than the original material. Further efforts will concentrate on purifying the major components to provide additional supporting evidence for the proposed intermediate structures and formation mechanism.

The formation of intermediate aggregates appears to be a general phenomenon for reactions at low initial proton to aniline ratio (<1.0). A reaction mechanism is proposed for the formation of these molecules. We speculate that tetramers are formed through cross-linking between oxidized dimers, *N*-phenyl quinonediimine (PQDI). Some minor components are also separated and identified, supporting the proposed mechanism. We believe that this work provides some new scientific insights into the chemical structures of the intermediates. The proposed reaction mechanism may explain the reaction pathways of the formation of intermediates. Clearly, additional work is needed to completely verify our proposed structures and reaction mechanism. We hope this study will spur additional investigation of this challenging reactive system.

Acknowledgment. We thank Dr. Ross E. Muenchausen (LANL, MST-8) for UV−Vis access and Dr. Debra Wrobleski (LANL, MST-7) for GPC access. We thank Dr. Weizhong Chen (LANL, C-IIAC) for advice on column chromatography and thin layer chromatography. We also thank Prof. Richard B. Kaner (UCLA) for thoughtful discussions. This work was mainly supported by the Laboratory Directed Research and Development Program at Los Alamos National Laboratory, and some supported by DOE EERE-ITP Program.

References and Notes

(1) Trivedi, D.; Dhawan, S. *J. Mater. Chem.* **1992**, *2*, 1091.
(2) DeBerry, D. W. *J. Electrochem. Soc.* **1985**, *132*, 1022.
(3) Mondal, S. K.; Munichandraiah, N. *J. Solid State Electrochem.* **2006**, *10*, 78.
(4) Janata, J.; Josowicz, M. *Nat. Mater.* **2003**, *2*, 19.
(5) Virji, S.; Kaner, R. B.; Weiller, B. H. *Chem. Mater.* **2005**, *17*, 1256.
(6) Sivaraman, P.; Hande, V. R.; Mishra, V. S.; Rao, C. S.; Samui, A. B. *J. Power Sources* **2003**, *124*, 351.
(7) Vinay, G.; Norio, M. *Electrochem. Solid-State Lett.* **2005**, *8*, A630.
(8) Huang, J.; Kaner, R. B. *Nat. Mater.* **2004**, *3*, 783.
(9) Tseng, R. J.; Huang, J.; Ouyang, J.; Kaner, R. B.; Yang, Y. *Nano Lett.* **2005**, *5*, 1077.
(10) MacDiarmid, A. G.; Yang, L.; Huang, W.; Humphrey, B. *Synth. Met.* **1987**, *18*, 393.

(11) MacDiarmid, A. G. Conducting Polymers as New Materials for Hydrogen Storage. In U.S. Department of Energy Presentation, Washington, D.C., May 16−19, 2006.
(12) Tran, H. D.; Li, D.; Kaner, R. B. *Adv. Mater.* **2009**, *21*, 1487.
(13) Wan, M. *Adv. Mater.* **2008**, *20*, 2926.
(14) Sapurina, I.; Stejskal, J. *Polym. Int.* **2008**, *57*, 1295.
(15) Surwade, S. P.; Agnihotra, S. R.; Dua, V.; Manohar, N.; Jain, S.; Ammu, S.; Manohar, S. K. *J. Am. Chem. Soc.* **2009**, *131*, 12528.
(16) Gospodinova, N.; Mokreva, P.; Terlemezyan, L. *Polymer* **1993**, *34*, 2438.
(17) Gospodinova, N.; Terlemezyan, L.; Mokreva, P.; Kossev, K. *Polymer* **1993**, *34*, 2434.
(18) Stejskal, J.; Sapurina, I.; Trchova, M.; Konyushenko, E. N. *Macromolecules* **2008**, *41*, 3530.
(19) Stejskal, J.; Sapurina, I.; Trchova, M.; Konyushenko, E.; Holler, P. *Polymer* **2006**, *47*, 8253.
(20) Ding, Z.; Yang, D.; Currier, R. P.; Obrey, S. J.; Zhao, Y. *Macromol. Chem. Phys.* **2010**, *211*, 627.
(21) Trchova, M.; Sedenkova, I.; Konyushenko, E. N.; Stejskal, J.; Holler, P.; Ciric-Marjanovic, G. *J. Phys. Chem. B* **2006**, *110*, 9461.
(22) *CRC Handbook of Chemistry and Physics*; 88th ed.; Lide, D. R., Ed.; CRC Press: Cleveland, OH, 2007−2008; p 8.
(23) MacDiarmid, A. G. *Angew. Chem., Int. Ed.* **2001**, *40*, 2581.
(24) Ding, Z.; Currier, R. P.; Zhao, Y. S.; Yang, D. *Macromol. Chem. Phys.* **2009**, *210*, 1600.
(25) Laslau, C.; Zujovic, Z. D.; Zhang, L.; Bowmaker, G. A.; Travas-Sejdic, J. *Chem. Mater.* **2009**, *21*, 954.
(26) Huang, W. S.; MacDiarmid, A. G. *Polymer* **1993**, *34*, 1833.
(27) Petr, A.; Wei, D.; Kvarnstrom, C.; Ivaska, A.; Dunsch, L. *J. Phys. Chem. B* **2007**, *111*, 12395.
(28) Willstatter, R.; Moore, C. W. *Ber.* **1907**, *40*, 2665.
(29) Cao, Y.; Li, S.; Xue, Z.; Guo, D. *Synth. Met.* **1986**, *16*, 305.
(30) Nalwa, H. S. *J. Mater. Sci.* **1991**, *26*, 1683.
(31) Venancio, E. C.; Wang, P.-C.; MacDiarmid, A. G. *Synth. Met.* **2006**, *156*, 357.
(32) Surwade, S. P.; Dua, V.; Manohar, N.; Manohar, S. K.; Beck, E.; Ferraris, J. P. *Synth. Met.* **2009**, *159*, 445.
(33) Zujovic, Z. D.; Laslau, C.; Bowmaker, G. A.; Kilmartin, P. A.; Webber, A. L.; Brown, S. P.; Travas-Sejdic, J. *Macromolecules* **2010**, *43*, 662.
(34) Zhu, Y.; Li, J.; Wan, M.; Jiang, L. *Polymer* **2008**, *49*, 3419.
(35) Yang, D.; Adams, P.; Goering, R.; Mattes, B. *Synth. Met.* **2003**, *135−136*, 293.
(36) Niu, Z.; Bruckman, M.; Kotakadi, V. S.; He, J.; Emrick, T.; Russell, T. P.; Yang, L.; Wang, Q. *Chem. Commun.* **2006**, 3019.
(37) Niu, Z.; Liu, J.; Lee, L. A.; Bruckman, M. A.; Zhao, D.; Koley, G.; Wang, Q. *Nano Lett.* **2007**, *7*, 3729.
(38) Alam, T.; Tarannum, H.; Ali, S. R.; Kamaluddin. *J. Colloid Interface Sci.* **2002**, *245*, 251.
(39) Lee, Y. M.; Kim, J. H.; Kang, J. S.; Ha, S. Y. *Macromolecules* **2000**, *33*, 7431.
(40) Kříž, J.; Starovoytova, L.; Trchovaí, M.; Konyushenko, E. N.; Stejskal, J. *J. Phys. Chem. B* **2009**, *113*, 6666.
(41) Cotarelo, M. A.; Huerta, F.; Mallavia, R.; Morallón, E.; Vázquez, J. L. *Synth. Met.* **2006**, *156*, 51.
(42) Okamoto, T.; Terada, E.; Kozaki, M.; Uchida, M.; Kikukawa, S.; Okada, K. *Org. Lett.* **2003**, *5*, 373.
(43) Sousa, M. M.; Melo, M. J.; Parola, A. J.; Morris, P. J. T.; Rzepa, H. S.; de Melo, J.; Sérgio, S. *Chem.—Eur. J.* **2008**, *14*, 8507.
(44) Melo, J. S. d.; Takato, S.; Sousa, M.; Melo, M. J.; Parola, A. J. *Chem. Commun.* **2007**, 2624.
(45) Meth-Cohn, O.; Smith, M. *J. Chem. Soc., Perkin Trans. I* **1994**, 5.
(46) Proevska, L. I.; Pojarlieff, I. G. *Dyes Pigm.* **1998**, *36*, 177.
(47) Izumi, C. M. S.; Constantino, V. R. L.; Temperini, M. L. A. *J. Phys. Chem. B* **2005**, *109*, 22131.
(48) Surwade, S. P.; Manohar, N.; Manohar, S. K. *Macromolecules* **2009**, *42*, 1792.
(49) Zhang, W. J.; Feng, J.; MacDiarmid, A. G.; Epstein, A. J. *Synth. Met.* **1997**, *84*, 119.
(50) Chen, L.; Yu, Y.; Mao, H.; Lu, X.; Zhang, W.; Wei, Y. *Mater. Lett.* **2005**, *59*, 2446.
(51) Kaczorowski, R.; Gosk, J.; Kulszewicz-Bajer, I.; Twardowski, A. *Synth. Met.* **2005**, *151*, 106.
(52) Tratnyek, P. G.; Reilkoff, T. E.; Lemon, A. W.; Scherer, M. M.; Balko, B. A.; Feik, L. M.; Henegar, B. D. *Chem. Ed.* **2001**, *6*, 172.
(53) Galasso, V. *Chem. Phys. Lett.* **2008**, *457*, 250.
(54) Fernández, R. O.; Pizarro, R. A. *J. Chromatogr., A* **1997**, *771*, 99.
(55) Niu, S.-Y.; Jiao, K. *Acta Chim. Sinica* **2000**, *58*, 617.
(56) Wheaton, G. A.; Stoel, L. J.; Stevens, N. B.; Frank, C. W. *Appl. Spectrosc.* **1970**, *24*, 339.

JP102623Z